12. Goswami, D. C., Brahmaputra River, Assam, India: Physiography, basin denudation and channel aggradation. *Water Resour. Res.*, 1985, **21**, 959–978.

13. Sarma, J. N., Fluvial process and morphology of the Brahmaputra river in Assam, India. *Geomorphology*, 2005, **70**, 226–256.

14. Lahiri, S. K. and Sinha, R., Morphotectonic evolution of the Majuli Island in the Brahmaputra valley of Assam, India inferred from geomorphic and geophysical analysis. *Geomorphology*, 2014, **227**, 101–111.

15. Lahiri, S. K. and Sinha, R., Tectonic controls on the morphodynamics of the Brahmaputra River system in the upper Assam valley, India. *Geomorphology*, 2012, **169–170**, 74–85.

16. Telford, W. M., Geldart, L. P. and Sheriff, R. E., *Applies Geophysics*, Cambridge University Press, 1990, 2nd edn.

Groundwater prospects in basaltic formations of Mangaon, Raigad district from electrical resistivity imaging technique

Gautam Gupta*, Vinit C. Erram, B. D. Kadam and M. Laxminarayana

Indian Institute of Geomagnetism, Kalamboli Highway, Navi Mumbai 410 218, India

A two-dimensional resistivity survey was conducted using the Wenner–Schlumberger configuration in the premises of Vijaya Gopal Gandhi Primary and Secondary Ashramshala, Utekhol in Mangaon, Maharashtra. Measurements of three profiles were studied with an aim to delineating the groundwater potential by studying the degree of weathering and fracturing in the weathered profile developed above the basement. The measured resistivity data were inverted using the RES2DINV software. Results from the 2D inverse models of resistivity variation with depth suggest the occurrence of potential aquifer mostly in weathered/fractured zones within the traps or below it. In addition, the resistivity models produced indicate the presence of saturated fracture zone that could be exploited for groundwater extraction. Vertical electrical sounding measurement using the Schlumberger arrangement was conducted at two locations, which substantiate the 2D model results.

GROUNDWATER, a natural and renewable resource, plays a crucial role in the socio-economic advancement of any region. The area under study is the hard rock terrain of Deccan Volcanic Province (DVP) in Maharashtra facing a major problem in terms of depletion of groundwater due to various reasons such as sporadic spatial and temporal distribution of precipitation. Thus it is pertinent to identify additional sources of groundwater for exploitation over the Deccan Traps covered region. The geophysical studies were carried out at the Vanavasi Kalyan Ashram, Vijaya Gopal Gandhi Primary and Secondary Ashramshala, Utekhol in Mangaon, Maharashtra. This residential school, which functions with the grant-in-aid from the Government of Maharashtra, is for the children of the local tribes as they are not able to take care of education of their children because of their nomadic and weak financial status. The school caters to about 450 students staying on a water-starved campus. Due to the inadequate supply of pipe-borne and surface water, it is essential to make alternate arrangement of water supply for the students. Attempts were made by other agencies in the past to drill bore wells in the campus, however, two bore wells failed to yield water and the third well yields less water but usually goes dry during summer.

Geophysical studies are regularly employed to assess the groundwater potential of an area. Though such studies provide a fast and cost-effective means to derive subsurface information, however at times, this is plagued with ambiguities and uncertainties in data interpretation[1]. The use of geophysical techniques for groundwater resource mapping has increased radically over the last couple of decades due to rapid strides in instrumentation and advanced numerical modelling solutions[2,3]. Although various geophysical methods exist, electrical resistivity is a widely used technique owing to its operational simplicity and effectiveness in areas with contrasting resistivity, such as between the weathered overburden and the bedrock[4].

One-dimensional (1D) vertical electrical soundings (VES) have been conventionally used to obtain a layered model of the subsurface and the depth to substratum. Nevertheless in many cases, the subsurface cannot judiciously be resolved into horizontal homogeneous layers with lateral resistivity variations as necessary for interpretation. In this study, two-dimensional (2D) electrical resistivity imaging (ERI) and VES surveys were carried out for assaying the depth and thickness of groundwater potential zones and to produce 2D resistivity models of the shallow subsurface in the basaltic hard rock formation within the premises of the school in Mangaon area. A

*For correspondence. (e-mail: ggupta@iigs.iigm.res.in)
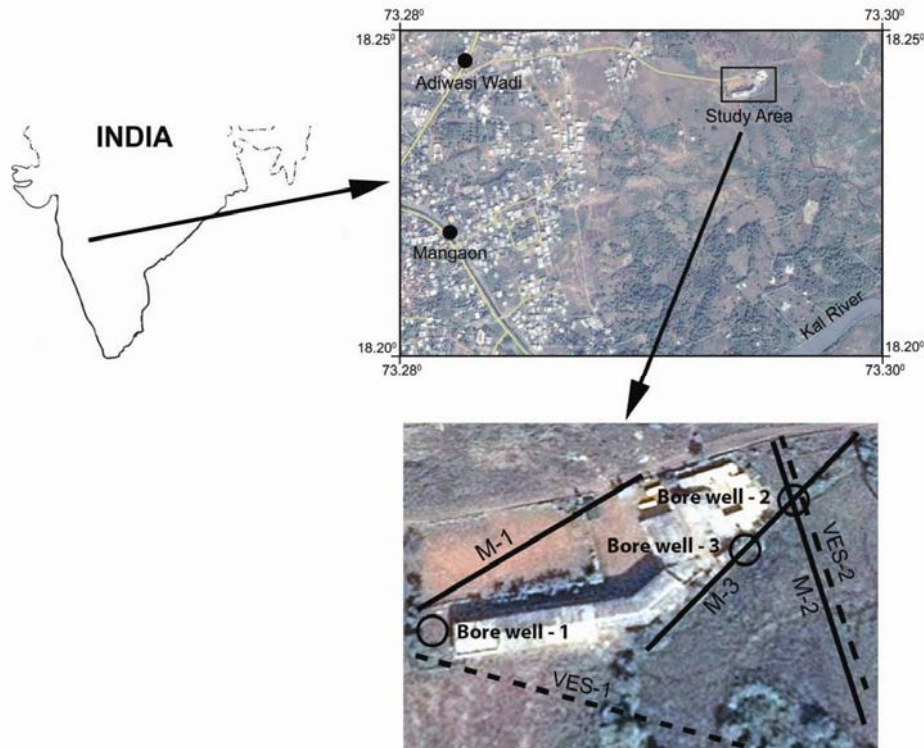
Figure 1. Location map of the study area showing the resistivity imaging profiles, vertical electrical sounding points and the bore wells.

total of three ERI and two VES profiles were surveyed in the school campus (Figure 1).

The entire study area is covered by Deccan basaltic formations consisting of horizontal lava flows of late Cretaceous to early Eocene. Simple basalt (aa type) and vesicular-amygdaloidal (compound pahoehoe) basalt flow are predominant in the area. Also red bole beds (Tachylitic bands) are exposed in the road cuts and well sections. Westerly flowing rivers and their tributaries with steep to moderate slope navigate the Mahad–Mangaon region[5]. The low land Mangaon basin, which is surrounded by hilly terrain, is oval shaped and numerous NS, NNW–SSE and EW lineaments criss-cross the region. This is indicative of the fact that the basin is bounded by faults and is a result of neotectonic activity[5].

The study area encompasses an area of about 500 sq. m. The region receives regular seasonal average rainfall of about 3500 mm annually. It is highly humid throughout the year. The mean minimum temperature is 17.7°C and the mean maximum temperature is 31.8°C (ref. 6). Groundwater occurs generally in the upper weathered and fractured parts up to depths of 10–15 m under unconfined conditions in Deccan Traps. At deeper levels, the groundwater-bearing strata occurs under semi-confined to confined conditions. The yield of dug wells tapping upper phreatic aquifer ranges between 45 and 60 m³/day, whereas that of bore wells varies from 0.50 to >20 m³/h depending upon the local hydrogeological con-

ditions, however in most of the borewells it is up to 5 m³/h. Water-bearing zones in Mangaon were encountered between the depth of 12 and 196 m bgl, thus suggesting that water-bearing zones exists even at deeper depths. The static water level ranges from 0.98 to more than 85 m bgl (ref. 6).

Several researchers have used the resistivity technique for a variety of applications including groundwater studies[7,8], groundwater contamination studies[9], saltwater intrusion problems[10] and geothermal explorations[11]. Systematic hydrogeological and geophysical studies have been undertaken in the past in the Deccan traps region[12–16] to delineate aquifers and the incidence of groundwater in intertrappeans/vesicular and fractured zones within the trap succession and sedimentary formations underneath the traps, which are supposed to be potential for groundwater.

The electrical resistivity method is based on the measurement of potential difference between a pair of potential electrodes, M and N at the surface resulting from a current flowing between a pair of current electrodes, A and B into the ground[17,18], which is used to measure the apparent resistivity (ρ_a). By increasing the current electrode separation, the depth of penetration can be increased, thus providing information about the subsurface formations.

The multi-electrode technique is a rapid computer-controlled data acquisition system, wherein both lateral and vertical resistivity variation beneath the profile

length is studied. Also due to large amount of data, the computed images of the subsurface structures are of higher resolution. The multi-electrode imaging scheme is extensively used in groundwater exploration, environmental and mining applications[19–21]. Thus, the use of resistivity imaging technique for groundwater exploration has earned an important place in recent years in spite of some interpretive constraint. It is thus expected that the results obtained from the present study would generate detailed groundwater scenario and locations within the school campus can be recommended for drilling tube wells/bore wells.

The multi-electrode resistivity procedure uses a multi-core cable with as many metal electrodes (24, 48, 72, 96…) embedded into the ground at a fixed spacing, every 5/10/15 m for example. The sequence of readings is pre-defined and stored in the internal memory of the resistivity data logger. The relays are located in the resistivity unit, which switches off those electrodes according to the sequence. Various combinations of current and potential pairs of electrodes create the geoelectric section, where the maximum depth of study depends on the total length of the cable[22].

The depth of penetration is related to the distance between electrodes and the geology of the area. For instance, if a set of 48 electrodes is spaced at 5 m (24 electrodes on either side of the resistivity meter), then the total length of the cables is 235 m. For Schlumberger and Wenner arrays, the maximum depth of study is about 20% of the total cable length. This depth is achieved for the combination of two extreme left and two extreme right electrodes of the profile, and plotting point relates to the bottom angle of the triangle of the resistivity pseudo section[22].
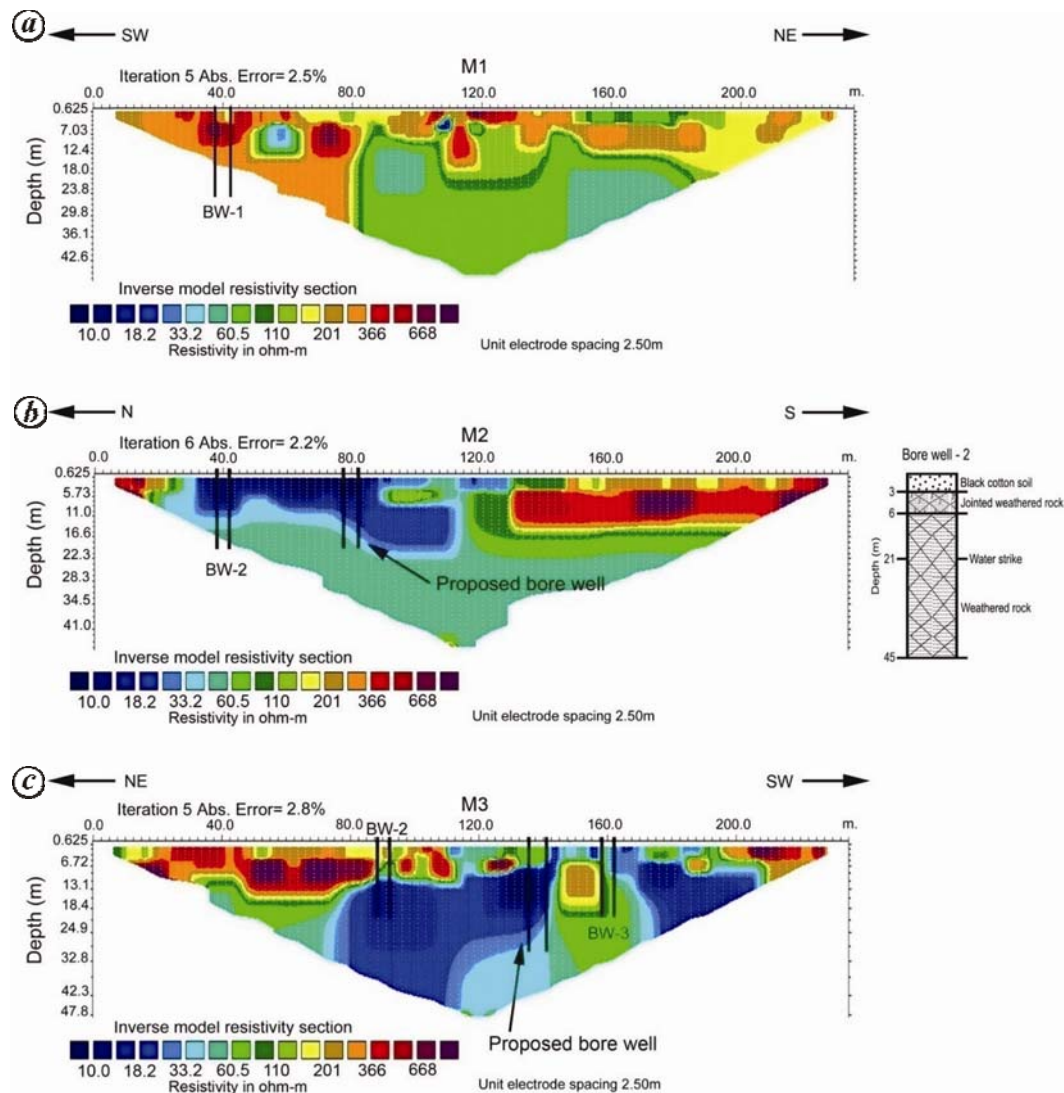
The Wenner–Schlumberger hybrid configuration has been used in this study. This configuration is moderately sensitive to both horizontal and vertical sub-structures. The average depth of study area is greater, while the signal strength is weaker than that of Wenner array. Also the penetration depth of this hybrid configuration is greater than that of dipole–dipole array and twice that of pole–dipole array, which results in a higher signal-to-noise ratio[23]. Electrical resistivity imaging was carried out at three stations (M1, M2 and M3) (Figure 1) in the school premises using SYSCAL R1plus switch 48 system (manufactured by IRIS, France) with 5 m inter-electrode separation. The total length of the profile is 235 m, ensuring a penetration depth of about 41–48 m. As the top layer in the study area is dry and hard, it was necessary to reduce the contact resistance between the electrodes and the ground before data acquisition. Thus the electrical coupling of the electrodes with the subsurface was improved by adding salt water to every electrode, resulting in a contact resistance below 2 KΩ (refs 24, 25).

2D inversion was performed using the software 'RES2DINV' version 3.54u, applying the smoothness-constrained least squares inversion by a complete Gauss–Newton optimization approach[22], as the number of model parameters is small thereby giving an exact and more realistic subsurface geological information. As the data set appears to be noisy, these artifacts could be significantly reduced using larger values for the damping factors[22]. In the present case, the initial and minimum damping factor used for inversion was 0.20 and 0.05 respectively, while the default setting is 0.160 and 0.015 respectively. As the resolution of the resistivity model decreases exponentially with depth, the damping factor was also accordingly increased by a factor of 1.05 with each deeper layer. The damping factor was optimized to obtain less number of iterations for the program to converge significantly; however, the time taken per iteration was more.

A response is calculated from the initial 2D electrical resistivity model produced, and compared with the measured apparent resistivity values of the field data[26]. The optimization method iterates and attunes the resistivity value of the model until the calculated apparent resistivity values of the model are in close conformity with the measured values of the field data[15]. The quality of the resistivity model is revealed by the absolute (ABS) error, which provides a measure of the differences between the model response and the measured data. Using this scheme, 2D inverted models of true resistivity variation of sub-surface formations for all the three sites have been computed. The final output is the 2D inverse model of true resistivity variation with depth. The noisy and erroneous data points were filtered by removing the resistivity values having negative voltage or with a standard deviation greater than 1%. The ABS error in the inverted models was in the 2.2–2.8% range. In order to reduce the distortion caused by large variations in resistivity near the ground surface to obtain improved results, an inversion model with width of the cells half the unit electrode spacing was used for all the three imaging profiles[22].

Profile M1 is trending in NE–SW direction and is located at the front of the school premises. The inverted resistivity model (Figure 2 a) reveals a rather heterogeneous sub-surface. The model converged after 5 iterations with a 2.5% ABS error. The western part of the profile up to 145 m lateral distance is highly resistive (>200 Ω-m), reflecting hard rock formation from shallow to deeper levels. However, at distances 50–60 m, a minor saturated zone is seen at depths of 7 m. Between distances 145 and 195 m, the sub-surface is characterized by relatively low resistivity ranging from about 60–110 Ω-m up to depths of about 7 m, which is underlain by high resistivity layer. At lateral distance 80–190 m, a wide low resistivity zone (about 33–110 Ω-m) is observed extending up to depth of probing, indicating fractured basalt saturated with water. Further east, beyond 195 m distance, the sub-surface is composed of hard rock formation having resistivity in excess of 200 Ω-m. The low resistive zone towards east beneath distance 80 m juxtaposed against a high resistive

Figure 2. *a*, Inverted resistivity model of profile M1 (using Wenner–Schlumberger configuration) in southwest–northeast direction. The resistivity model is obtained using complete Gauss–Newton optimization technique with an electrode spacing of 2.5 m, iteration 5 and ABS error 2.5%. *b*, Inverted resistivity model of profile M2 (using Wenner–Schlumberger configuration) in north–south direction. The resistivity model is obtained using complete Gauss–Newton optimization technique with an electrode spacing of 2.5 m, iteration 6 and ABS error 2.2%. *c*, Inverted resistivity model of profile M3 (using Wenner–Schlumberger configuration) in northeast–southwest direction. The resistivity model is obtained using complete Gauss–Newton optimization technique with an electrode spacing of 2.5 m, iteration 5 and ABS error 2.8%.

zone towards west is perhaps controlled by a lineament passing in the vicinity beneath 80 m horizontal distance. A bore well (BW1) was drilled prior to the geophysical survey, at distance 40 m on the western part of the resistivity imaging profile. The drilling was terminated at 40 m depth, as no viable water was found. The resistivity model also suggests that the region beneath BW1 comprises hard rock and no aquifer zone is visible. A probable locale of potential groundwater zone could be at lateral distance 90–160 m. This location however may not be feasible because it is right at the front of the main school building, thus causing hindrance to regular movement of the residents.

The resistivity profile (M2) was undertaken at the rear side of the school building trending in NS direction. The

inverse resistivity model (Figure 2 *b*) was obtained after six iterations with an ABS error of 2.2%. The model suggests that the top 15–20 m is conductive to the north whereas the top 15 m is highly resistive to the south over the profile. A sub-horizontal conductive (about 18 Ω-m) layer is revealed at 40 m lateral distance, continuing up to depth of probing, which may be a clay-dominated zone saturated with water. In the trap areas, at times clay-rich sediments are deposited in the form of intertrappeans, known as bole beds[27], which are not a prospective groundwater zone.

Between lateral distances 80 and 110 m, this zone is delineated up to depth of about 20 m. Further south, at lateral distance 120–235 m, the top 15 m is resistive (>100 Ω-m). Underneath the top 15–20 m, the sub structure
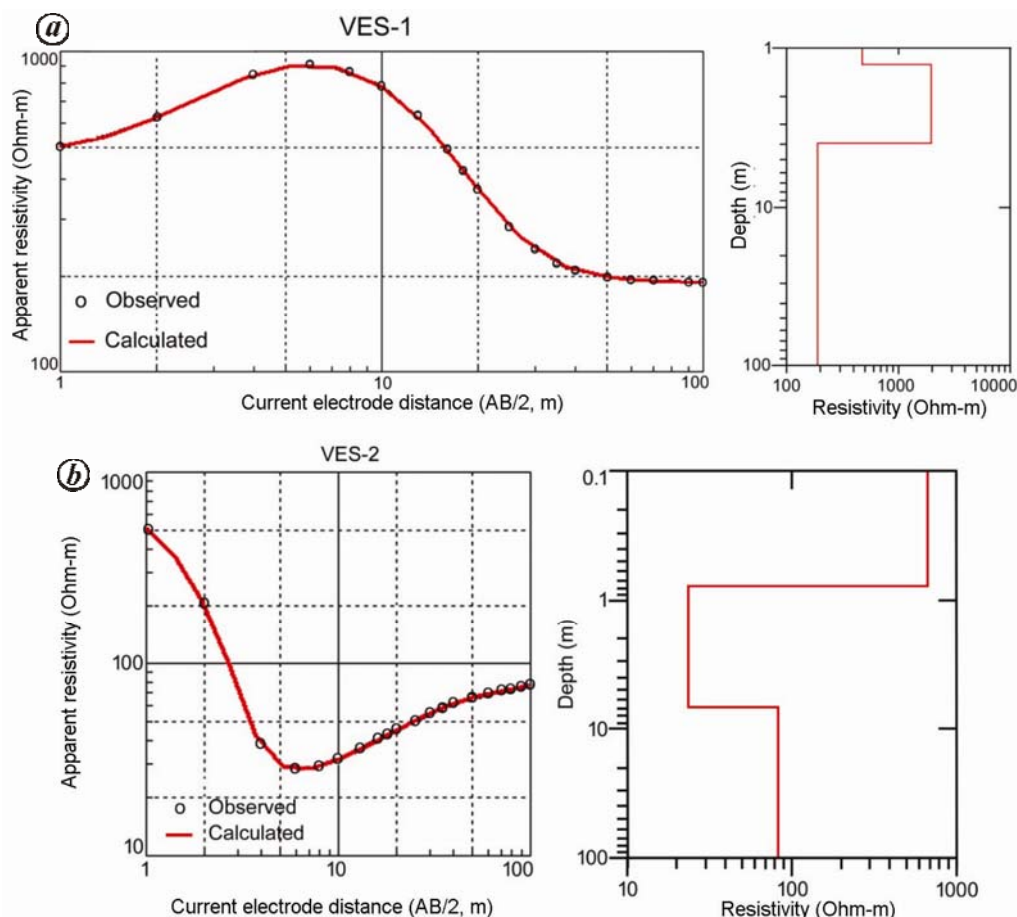
Figure 3. *a*, Vertical electrical sounding curve of station 1. Also shown is the resistivity versus depth model for VES-1. *b*, Vertical electrical sounding curve of station 2. Also shown is the resistivity versus depth model for VES 2.

is homogeneous throughout the profile and has resistivity value of about 50–60 Ω-m symptomatic of weathered rock. A bore well (BW2) was drilled prior to this survey and the point of BW2 coincided at 40 m lateral distance of the resistivity profile. The lithology of BW2, given adjacent to Figure 2 *b*, implies that the top 3 m consists of black cotton soil. Underlying this, a 3 m thick layer of jointed weathered rock is obtained. Up to depths of 45 m, the lithology consists of weathered rock. The BW2 litholog corroborates well with the resistivity model, at least up to depths of penetration. At present BW2 yields copious amount of water, which however is meagre during the summer months. It is expected that if the depth of BW2 is increased, the yield may improve even during summer. Alternately, a new bore well may be drilled at lateral distance 90 m to tap the deeper aquifer for auxiliary source of water.

The imaging profile (M3) was carried out in a northeast–southwest trend just at the rear of the school building. The inverse resistivity model converged after five iterations with an ABS error of 2.8%. The resistivity profile coincides with BW2 at 90 m and another bore well (BW3) at 160 m horizontal distance. The inverted resis-

tivity model (Figure 2 *c*) depicts that the sub surface is highly heterogeneous in nature. High resistivity zone comprising of hard and compact basalt is seen up to lateral distance of 80 m in the northeastern part of the profile. This zone has resistivity values in excess of 200 Ω-m up to depths of about 15 m. At horizontal distance 90–130 m, a broad low resistive (18–33 Ω-m) zone is seen. The low resistive zone beneath distance 90 m corresponds to BW2, while the low resistive zone beneath 130 m distance also reveals a weathered zone. Beneath 145–155 m lateral distances, a high resistive block is observed having resistivity value greater than 200 Ω-m and thickness of about 10 m. Beneath this, fractured rocks are prevalent with resistivity values of the order of 60 Ω-m up to depth of probing. As mentioned earlier, BW3 coincides with this zone at lateral distance 160 m. Initially this bore well was yielding water but with time, the yield was less and presently BW3 is dry.

On the southwestern part, a low resistive zone is revealed at lateral distance 160–200 m from shallow depth up to depth of penetration. This feature reflects a resistivity value in the 18 Ω-m range, indicating saturated clayey layer. Further west beyond 200 m distance, the

Table 1. Summary of VES interpretation

	Layer resistivity (Ωm)			Thickness (m)		Total thickness d (m)	RMS error (%)
	$\rho 1$	$\rho 2$	$\rho 3$	h1	h2		
VES 1	474	1977	188	1.26	2.66	3.92	0.346
VES 2	674	23.7	84.3	0.79	6.14	6.93	0.848

subsurface is composed of hard rock formation having resistivities greater than 200 Ω-m.

As mentioned earlier, two Schlumberger soundings (AB/2 = 100 m) were also conducted in the school campus to provide 1-D layered information (Figure 1).

Interpretation of both the resistivity soundings[28] is shown in Figure 3. The resistivities and thicknesses of different layers of interpreted models are depicted alongside the figure. A good corroboration is seen between the observed and model data for both the soundings wherein RMS error of 0.346% and 0.848% respectively was obtained. VES1 was acquired in a NW–SE trend at the rear side of the school building, whereas VES2 was along the profile of M2 (Figure 1). Table 1 gives the summary of VES interpretation.

Interpretation of resistivity sounding VES1 (Figure 3 *a*) reveals the top layer to be highly resistive (about 500 Ω-m) having a thickness of about 1.2 m, presumably due to hard rock formation at the top. This overlies an even higher resistive formation having resistivity value in excess of 1900 Ω-m and thickness of about 2.6 m. The third layer is relatively conductive (resistivity of 188 Ω-m). This layer is likely to be jointed basalt, but is not favourable for groundwater due to its very shallow depth levels.

The location of VES2 corresponds to the resistivity imaging profile (M2). This location was chosen because of the prevailing hydrogeological conditions. The apparent resistivity curve revealed three layers. The top thin layer (about 0.79 m thick) revealed high resistivity value of 674 Ω-m, suggesting hard formation at the surface. This was followed a very low resistive feature having resistivity value of the order of 24 Ω-m having a thickness of about 6 m. This is the saturated clayey zone. The third layer is resistive (resistivity of about 84 Ω-m), indicative of the fact that formation up to depths of study is fractured. As mentioned earlier that over imaging profile M2 at lateral distance 80 m, an aquifer zone was delineated at depths of about 20 m beneath which weathered rock is encountered. Thus it can be surmised that the location of VES2 is ideal for construction of a shallow bore well.

From the present study, it is clear that both resistivity imaging and sounding results revealed the highly complex hydrogeological setting of the study area. These studies also identified potential aquifer zones in such a geologically complex setting. Resistivity models generated by inverse modelling of measured apparent resistivity data signify potential groundwater aquifers at lateral distances 40 and 80 m over profile M2, wherein fractured

and weathered rocks are predominant at depths beneath 20 m. The lithology of the bore well (BW2) also supports the resistivity model. Also, VES2 result indicates that the low resistivity obtained at depths of 6 m and below is conducive for groundwater extraction. This zone coincides with the low resistivity precinct observed at distance 80 m over profile M2. Thus this spot can be considered to drill a bore well, which could sustain the school's water requirements.

1. Kearey, P. and Brooks, M., *An Introduction to Geophysical Exploration*, ELBS, Blackwell Scientific Publication, Oxford, 1988, p. 296.
2. Muchingami, I., Hlatywayo, D. J., Nel, J. M. and Chuma, C., Electrical resistivity survey for groundwater investigations and shallow subsurface evaluation of the basaltic-greenstone formation of the urban Bulawayo aquifer. *Phys. Chem. Earth*, 2012, **50–52**, 44–51.
3. Rai, S. N., Thiagarajan, S., Shankar, G. B. K., Sateesh Kumar, M., Venkatesam, V., Mahesh, G. and Rangarajan, R., Groundwater prospecting in Deccan traps covered Tawarja basin using electrical resistivity tomography. *J. Ind. Geophys. Union*, 2015, **19**(3), 256–269.
4. Telford, W. M., Geldart, L. P. and Sheriff, R. E., *Applied Geophysics*, Cambridge University Press, 2nd edn, 1990.
5. Ubale, P. P., Geological aspects for the Konkan coastal belt area, around Mahad, Maharashtra. *Geosci. Res.*, 2012, **3**(1), 76–82.
6. Gupta, S., Groundwater information, Raigarh district, Maharashtra, CGWB Technical Report No. 1617/DB/2009, Ministry of Water Resources, Central Ground Water Board, Central region, Nagpur, 2009.
7. Gupta, G., Erram, V. C. and Kumar, S., Temporal geoelectric behavior of dyke aquifers in northern Deccan Volcanic Province, India. *J. Earth Syst. Sci.*, 2012, **121**(3), 723–732.
8. Kumar, D., Rai, S. N., Thiagarajan, S. and Ratnakumari, Y., Evaluation of heterogeneous aquifers in hard rocks from resistivity sounding data in parts of Kalmeshwar Taluk of Nagpur district, India. *Curr. Sci.*, 2014, **107**(7), 1137–1145.
9. Mondal, N. C., Singh, V. P. and Ahmed, S., Delineating shallow saline groundwater zones from Southern India using geophysical indicators. *Environ. Monit. Assess.*, 2013, **185**, 4869–4886.
10. Maiti, S., Gupta, G., Erram, V. C. and Tiwari, R. K., Delineation of shallow resistivity structure around Malvan, Konkan region, Maharashtra by neural network inversion of vertical electrical sounding measurements. *Environ. Earth Sci.*, 2013, **68**, 779–794; doi: 10.1007/s12665-012-1779-8.
11. Kumar, D., Thiagarajan, S. and Rai, S. N., Deciphering geothermal resources in Deccan Trap region using electrical resistivity tomography technique. *J. Geol. Soc. India*, 2011, **78**, 541–548.
12. Bose, R. N. and Ramkrishna, T. S., Electrical resistivity surveys for ground water in the Deccan trap country of Sangli district, Maharashtra. *J. Hydrol.*, 1978, **38**, 209–221.
13. Singhal, B. B. S., Hydrogeological characteristics of Deccan trap formations of India. In *Hard Rock Hydrosystems*, IAHS Publ. No. 241, 1997, pp. 75–80.

14. Pawar, N. J., Pawar, J. B., Supekar, A., Karmalkar, N. R., Kumar, S. and Erram, V. C., Deccan dykes as discrete and prospective aquifers in parts of Narmada-Tapi zone, Dhule District, Maharashtra. In *Indian Dykes* (eds Srivastava, R. K., Sivaji, Ch. and Chalapathi Rao, N. V.), Narosa Publishing House Pvt Ltd, New Delhi, 2009, pp. 189–198.

15. Ratnakumari, Y., Rai, S. N., Thiagarajan, S. and Dewashish Kumar, 2D Electrical resistivity imaging for delineation of deeper aquifers in a part of the Chandrabhaga river basin, Nagpur District, Maharashtra, India. *Curr. Sci.*, 2012, **102**(1), 61–69.

16. Rai, S. N., Thiagarajan, S., Ratnakumari, Y., Anand Rao, V. and Manglik, A., Delineation of aquifers in basaltic hard rock terrain using vertical electrical soundings data. *J. Earth Syst. Sci.*, 2013, **122**(1), 29–41.

17. Van Norstrand, R. and Cook, K. L., Interpretation of resistivity data, USCGS Professional Paper-499, US Govt. Printing Office, Washington, 1966.

18. Ritz, M., Parisot, J.-C., Diouf, S., Beauvais, A., Dione, F. and Niang, M., Electrical imaging of lateritic weathering mantles over granitic and metamorphic basement of eastern Senegal, West Africa. *J. Appl. Geophys.*, 1999, **41**, 335–344.

19. Dutta, S., Krishnamurthy, N. S., Arora, T., Rao, V. A., Ahmed, S. and Baltassat, J. M., Localization of water bearing fractured zones in a hard rock area using integrated geophysical techniques in Andhra Pradesh, India. *Hydrogeol. J.*, 2006, **14**, 760–766.

20. Krishnamurthy, N. S., Ananda Rao, V., Dewashish Kumar, Singh, K. K. K. and Shakeel Ahmed, Electrical resistivity imaging technique to delineate coal seam barrier thickness and demarcate water filled voids. *J. Geol. Soc. India*, 2009, **73**, 639–650.

21. Kumar, D., Rao, V. A., Nagaiah, E., Raju, P. K., Mallesh, D., Ahmeduddin, M. and Ahmed, S., Integrated geophysical study to decipher potential groundwater and zeolite-bearing zones in Deccan Traps. *Curr. Sci.*, 2010, **98**(6), 803–814.

22. Loke, M. H., Electrical imaging surveys for environmental and engineering studies – a practical guide to 2-D and 3-D surveys. Penang, Malaysia, 2011, http://www.geoelectrical.com/coursenotes.zip.

23. Dahlin, T. and Zhou, B., A numerical comparison of 2D resistivity imaging with ten electrode arrays. *Geophys. Prospect.*, 2004, **52**, 379–398.

24. Zarroca, M., Linares, R., Roqué, C., Rosell, J. and Gutiérrez, F., Integrated geophysical and morphostratigraphic approach to investigate a coseismic (?) translational slide responsible for the destruction of the Montclús village (Spanish Pyrenees). *Landslides*, 2014; doi: 10.1007/s10346-013-0427-z.

25. Loke, M. H. and Barker, R. D., Rapid least-squares inversion of apparent resistivity pseudosections by a quasi-Newton method. *Geophys. Prospect.*, 1996, **44**, 131–152.

26. Sasaki, Y., Resolution of resistivity tomography inferred from numerical simulation. *Geophys. Prospect.*, 1992, **40**, 453–463.

27. Deolankar, S. B., The Deccan Basalt of Maharashtra, India – their potential as aquifers. *Groundwater*, 1980, **18**(5), 434–437.

28. Bobachev, A., Resistivity sounding interpretation, IPI2WIN: Version 3.0.1, a 7.01.03, 2003, Moscow State University.

Multiplex-PCR assay for detection of some major virulence genes of *Salmonella enterica* serovars from diverse sources

Mridusmita Choudhury[1,2]**, Probodh Borah**[1,3,*]**,
Hridip Kumar Sarma**[2]**, Luit Moni Barkalita**[3]**,
Naba Kumar Deka**[1]**, Isfaqul Hussain**[4,5] **and
Md. Iftikar Hussain**[1,2]

[1]State Biotechnology Hub, Assam, College of Veterinary Science, Guwahati 781 022, India
[2]Department of Biotechnology, Gauhati University, Guwahati 781 014, India
[3]Department of Animal Biotechnology, and
[4]Department of Microbiology, College of Veterinary Science, Khanapara 781 022, India
[5]Faculty of Veterinary Microbiology and Immunology, Sher-e-kashmir University of Agricultural Sciences and Technology of Kashmir 190 006, India

The virulence of *Salmonella* depends on virulence factors encoded by specific genes. The present study describes the development of a simple and rapid multiplex PCR (m-PCR) assay for simultaneous detection of seven major virulence genes of *Salmonella* (*inv*A, *inv*H, *stn*, *sop*B, *sop*E, *sef*C and *pef*A). Presence of these genes was studied using 17 standard cultures and 76 field isolates from different sources. Seventeen non-*Salmonella* strains were also tested for specificity of the optimized PCR. A spiked control experiment was done to detect the sensitivity of m-PCR assay. The primer pairs were found to be specific for *Salmonella* only. The assay detected 250 pg of purified chromosomal DNA, or 12 cfu of *Salmonella* in crude lysates. All the field isolates and standard strains of *Salmonella* were found to carry *inv*A, *inv*H, *stn* and *sop*B genes, while variability was observed with respect to *sop*E, *sef*C and *pef*A genes. Thus this multiplex PCR assay provides a simple and rapid method for detection of major virulence factors in important clinical serovars of *Salmonella*.

Keywords: Multiplex PCR, *Salmonella*, spiking, virulence genes.

SALMONELLA, the Gram-negative bacillus of family Enterobacteriaceae, is widely distributed in nature and can cause diseases ranging from gastroenteritis to typhoid fever. More than 2500 serovars of *Salmonella* are known so far. *Salmonella enterica* subsp. *enterica* is one of the leading causes of zoonotic food-borne disease worldwide[1]. *Salmonella* infections exhibit a complex pathogenesis in which numerous virulence genes are involved[2]. These genes are clustered within *Salmonella* pathogenicity